

Supporting Information for

“*RAD21* promotes oncogenesis and lethal progression of prostate cancer”

Xiaofeng A. Su, Konrad H. Stopsack, Daniel R. Schmidt, Duanduan Ma, Zhe Li, Paul A. Scheet, Kathryn L. Penney, Tamara L. Lotan, Wassim Abida, Elise G. DeArment, Kate Lu, Thomas Janas, Sofia Hu, Matthew G. Vander Heiden, Massimo Loda, Monica Boselli, Angelika Amon, Lorelei A. Mucci

Corresponding Author: Xiaofeng A. Su.
Email : xsu@cpdr.org

This PDF file includes:

Table S1-S3.

Figure S1-S7.

Supporting text

SI references

Table S1. Expression in tumor and normal tissue, and difference (95% confidence interval), in arbitrary units (comparable between genes), for the 20 genes with the largest difference and *RAD21*.

Rank	Gene	Tumor	Normal	Difference
1	<i>TRIB1</i>	5.33	4.52	0.82 (0.69, 0.94)
2	<i>MAL2</i>	5.04	4.25	0.79 (0.66, 0.92)
3	<i>SNORA40</i>	8.83	8.24	0.58 (0.47, 0.70)
4	<i>TP53INP1</i>	5.12	4.57	0.55 (0.44, 0.66)
5	<i>MYC</i>	5.27	4.73	0.55 (0.45, 0.65)
6	<i>TPD52</i>	5.68	5.15	0.52 (0.41, 0.64)
7	<i>SNORD5</i>	8.86	8.33	0.52 (0.42, 0.62)
8	<i>PTP4A3</i>	6.06	5.55	0.51 (0.41, 0.61)
9	<i>FABP5</i>	4.83	4.32	0.51 (0.34, 0.68)
10	<i>SNORD54</i>	3.93	3.44	0.49 (0.37, 0.61)
11	<i>ESRP1</i>	5.13	4.64	0.49 (0.39, 0.59)
12	<i>ZFAND1</i>	4.34	3.90	0.43 (0.32, 0.55)
13	<i>GRHL2</i>	5.15	4.75	0.40 (0.29, 0.52)
14	<i>LYPLA1</i>	3.89	3.50	0.39 (0.31, 0.47)
15	<i>SLC10A5</i>	2.13	1.76	0.37 (0.25, 0.49)
16	<i>RIPK2</i>	4.32	3.96	0.36 (0.29, 0.43)
17	<i>NCALD</i>	3.52	3.16	0.36 (0.25, 0.47)
18	<i>RPL7</i>	8.34	8.00	0.34 (0.27, 0.41)
19	<i>FAM84B</i>	3.37	3.03	0.34 (0.26, 0.41)
20	<i>TSTA3</i>	3.88	3.56	0.32 (0.25, 0.39)
98	<i>RAD21</i>	4.46	4.36	0.10 (0.02, 0.18)

Table S2. Characteristics of patients with tumor–normal sequencing, MSK-IMPACT Clinical-Genomic Database, sequenced 2014–2020, by oncogenic *RAD21* alterations. Shown are count (percent) or median (interquartile range).

	By <i>RAD21</i> status	
	Intact	<i>RAD21</i> altered
<i>N</i>	2,504	88
Age at diagnosis (years)	63.2 (56.7, 68.8)	64.2 (56.7, 70.8)
Age at sample (years)	65.7 (59.3, 72.1)	68.2 (62.4, 74.9)
Diagnosis to sample (months)	2.4 (0.0, 35.4)	11.8 (0.0, 62.0)
Diagnosis to sequencing (months)	22.2 (5.5, 77.6)	27.7 (5.2, 79.4)
Self-reported race		
Asian	76 (3%)	3 (4%)
White	2,095 (89%)	70 (83%)
Black	194 (8%)	11 (13%)
Unknown	139	4
PSA at diagnosis (ng/ml)	9.0 (5.4, 26.8)	13.6 (6.2, 51.0)
Unknown	155	7
Gleason score		
<7	196 (9%)	8 (11%)
3+4	372 (16%)	8 (11%)
4+3	392 (17%)	13 (18%)
8	455 (20%)	10 (14%)
9-10	879 (38%)	34 (47%)
Unknown	210	15
Stage M1 at diagnosis	712 (28%)	34 (39%)
Sample tissue		
Prostate	1,684 (67%)	34 (39%)
Lymph node	345 (14%)	24 (27%)
Bone	259 (10%)	16 (18%)
Visceral	140 (6%)	10 (11%)
Other soft tissue	76 (3%)	4 (5%)
Extent of disease at sequencing		
Localized	693 (28%)	9 (10%)
Regional nodes	322 (13%)	11 (12%)
Metastatic hormone-sensitive	775 (31%)	31 (35%)
Non-metastatic castration-resistant	33 (1%)	0 (0%)
Metastatic castration-resistant	671 (27%)	36 (41%)
Metastatic, variant histology	10 (0%)	1 (1%)
Oncogenic <i>MYC</i> alteration	77 (3%)	67 (76%)
Chromosome arm 8q gain	738 (37%)	64 (88%)
Unknown	491	15

Table S3. Organoid growth conditions and antibodies.

Tab-1: Growth Condition

Medium: Advanced DMEM/F-12 (Thermo Fisher: 12634010) supplemented with HEPES (10mM), 2mM GlutaMAX and 1xpenicillin/streptomycin			
Additive factors	Vendor	Catelog #	Final concentration
B27	Thermo Fisher	17504044	50xdilution
N-acetylcystein	Sigma-aldrich	A7250-10G	1.25mM
EGF	VWR	10788-228	50ng/mL
Noggin	PeptoTech	250-38-20ug	100ng/mL
R-spondin 1	PeptoTech	315-32	500ng/mL
A83-01	Cayman	9001799	200nM
DHT	Sigma-aldrich	D-073-1ML	1nM
Y-27632 dihydrochloride	Cayman	10005583	10 μ M

Tab-2: Antibodies

Antibodies	Source	Identifier (RRID)	Type	Dilution	Experiment
Anti-RAD21	Millipore sigma	AB_417383	Primary	1:1000 or 1:500	WB
Phospho-Histone H2A.X (Ser139) Antibody	Cell Signaling Technology	AB_2118010	Primary	1:1000 for WB; 1:200 for IF	WB; IF
Recombinant Anti-ERG antibody [EPR3864]	Abcam	AB_2905642	Primary	1:1000	WB
Cleaved Caspase-3 (Asp175) Antibody	Cell Signaling Technology	AB_2341188	Primary	1:1000 for WB; 1:200 for IF	WB; IF
Phospho-Akt (Ser473) (D9E)	Cell Signaling Technology	RRID:AB_2315049	Primary	1:1000	WB
Anti-Cytokeratin 8 antibody [EP1628Y] (ab53280)	Abcam	AB_2890924	Primary	1:200	IHC
Anti-p63 antibody [4A4]	Abcam	AB_1006051	Primary	1:200	IHC
Androgen Receptor Polyclonal Antibody	Thermo Fisher Scientific	AB_325809	Primary	1:100	IF
GAPDH Antibody (G-9)	Santa Cruz Biotechnology	AB_10847862	Primary	1:1000	WB
alpha Tubulin Monoclonal Antibody (YL1/2)	Thermo Fisher Scientific	AB_2210201	Primary	1:1000	WB
Vinculin	Sigma-Aldrich	AB_477629	Primary	1:1000	WB
Donkey Anti-Mouse IgG (H+L) Antibody, Alexa Fluor 488 Conjugated	Invitrogen	AB_141607	Secondary	1:400	IF
Goat anti-Rabbit IgG (H+L) Cross-Adsorbed Secondary Antibody, Alexa Fluor 546	Invitrogen	AB_2534077	Secondary	1:400	IF
Goat anti-Rabbit IgG (H+L) Cross-Adsorbed Secondary Antibody, Alexa Fluor™ 488	Thermo Fisher Scientific	AB_143165	Secondary	1:400	IF
DyLight 800 Goat Anti-Rat IgG	BioRad	AB_2556604	Secondary	1:10000	WB
Anti-mouse IgG (H+L) (DyLight™ 680 Conjugate)	Cell Signaling Technology	AB_614942	Secondary	1:10000	WB
Anti-rabbit IgG (H+L) (DyLight™ 800 4X PEG Conjugate)	Cell Signaling Technology	AB_2556775	Secondary	1:10000	WB
WB: Western blot					
IF: immunofluorescence					
IHC: immunohistochemistry					

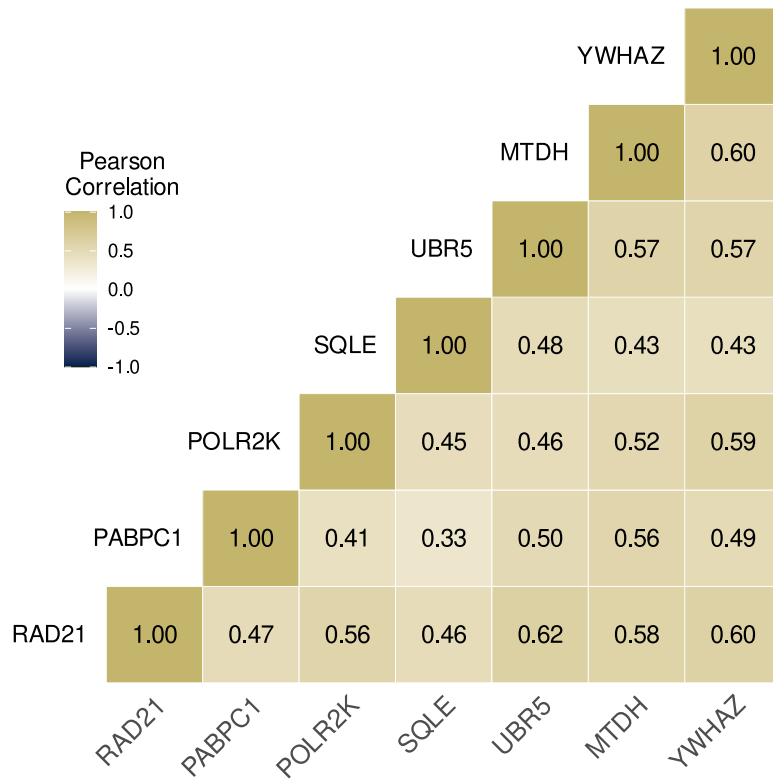


Figure S1. Pearson correlation between tumor mRNA expression levels of chr8q genes most strongly associated with risk of lethal prostate cancer (OR > 2).

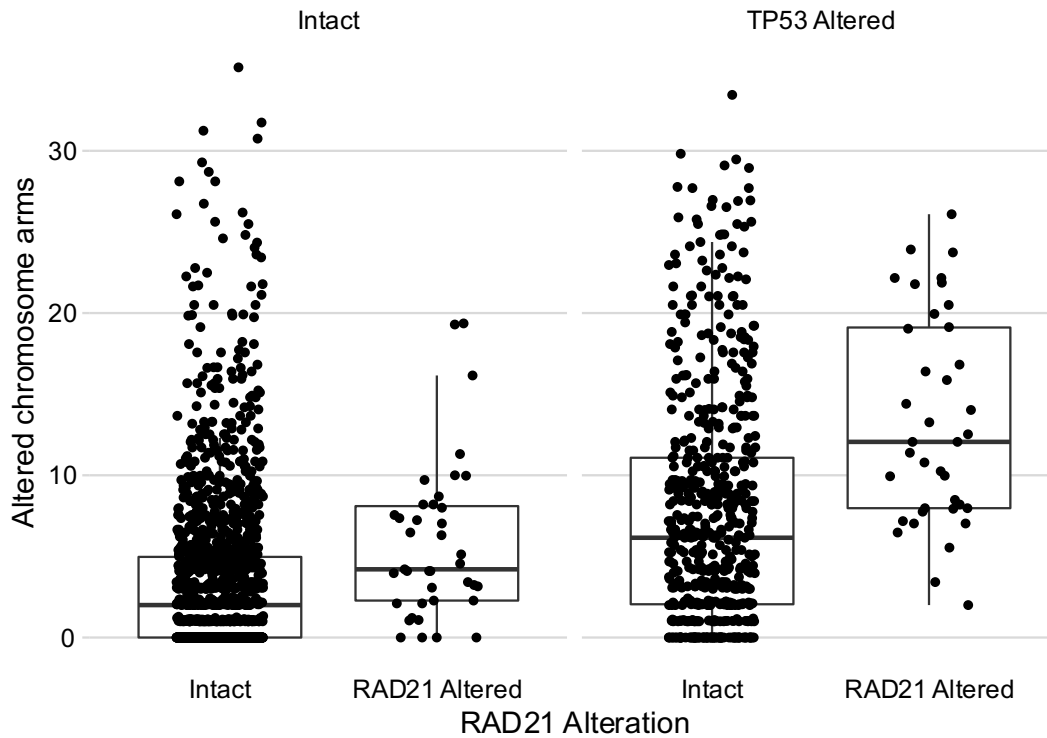


Figure S2. Counts of predicted altered chromosome arms by oncogenic RAD21 alterations and oncogenic *TP53* alterations, MSK-IMPACT Prostate Clinical-Genomic Database ($n = 2,592$), sequenced 2014–2020. Boxes indicate interquartile ranges, whiskers extend 1.5 times the interquartile range, thick horizontal lines indicate the median.

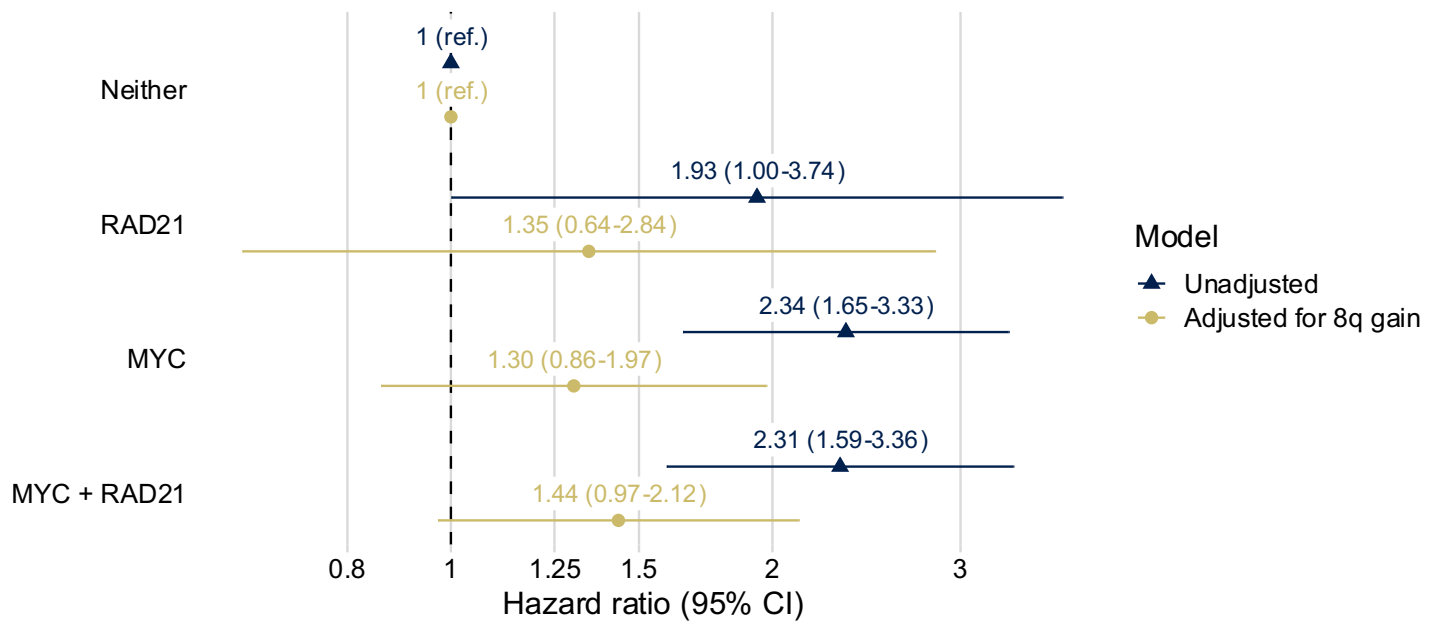


Figure S3. Association of oncogenic *RAD21* and *MYC* alterations with overall survival, MSK-IMPACT Prostate Clinical-Genomic Database, with survival follow-up 2014–2021, based on 38 deaths among the 88 patients with *RAD21*-altered tumors and 614 deaths among the 2,504 patients with *RAD21*-intact tumors. This joint classification by *RAD21* and *MYC* complements the estimate for *RAD21* alone shown in the main text.

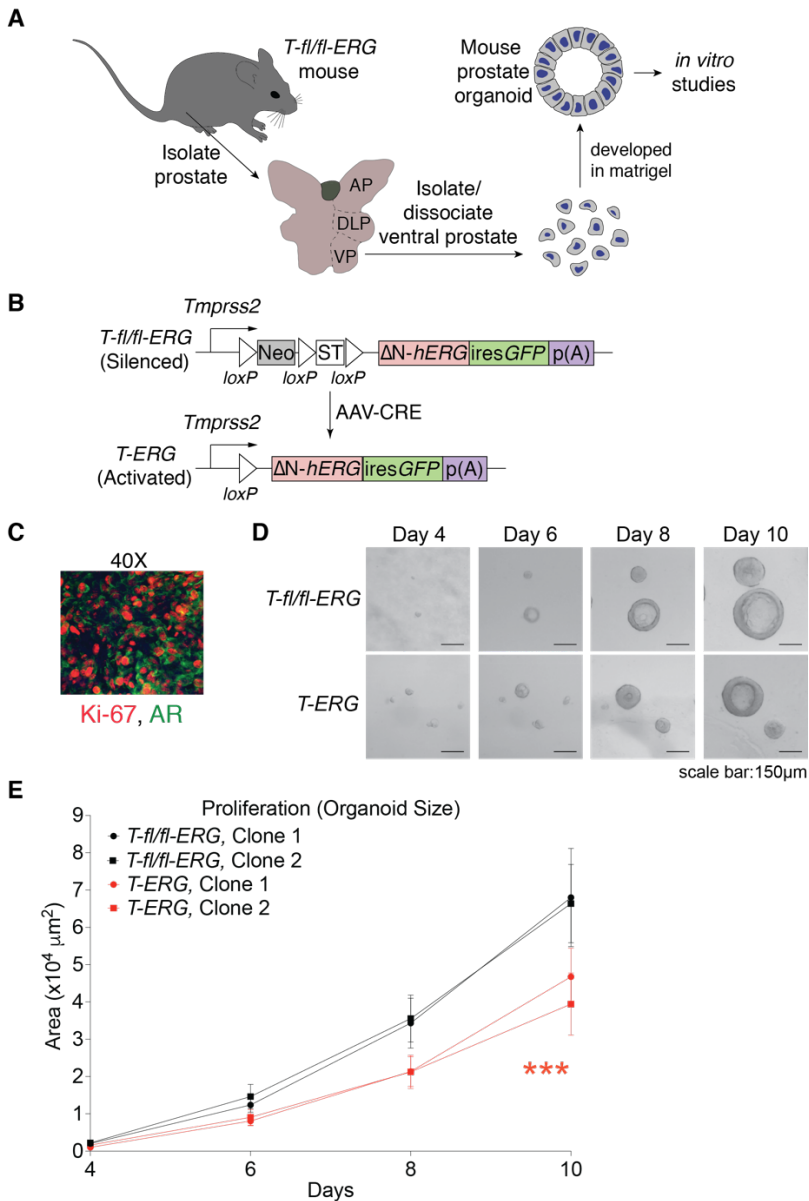
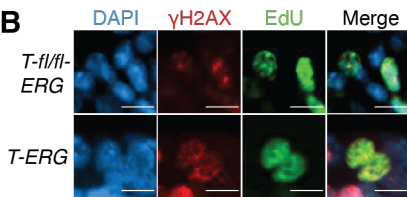
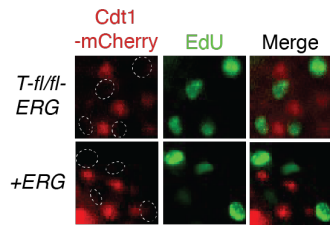
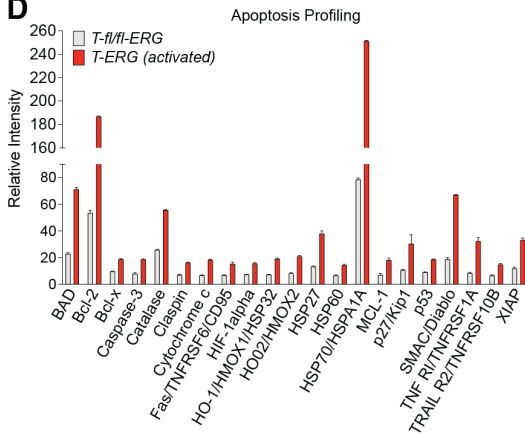


Figure S4. Growth of primary prostate organoids. (A) Scheme of development of primary prostate organoids. A mouse prostate was harvested from a mouse carrying an inducible *Tmprss2-fl/fl-ERG* (*T-fl/fl-ERG*) fusion. AP: anterior prostate; DLP: dorsolateral prostate; VP: ventral prostate. (B) Induction of T-ERG expression by Cre-mediated excision. AAV-Cre: adeno-associated virus containing Cre recombinase driven by a CMV promoter. (C) A wild-type mouse prostate organoid expresses both the proliferative marker, Ki67 (in red) and the prostatic marker, androgen receptor (AR, in green). Images were taken using a spinning disk confocal microscope with 40X objective magnification. (D, E) Proliferation measured by organoid size over time. 400 cells were seeded, and example time-lapse pictures are shown in (D). Quantification is in (E). Each dot represents an average over 18 independently growing organoids, with 95% confidence interval (CI) (error bar), at each indicated timepoint. *** $p < 0.001$, Linear regression comparing slopes between *T-fl/fl-ERG* and *T-ERG*.

A

RANK	TOP 20 Enriched GSEA Pathways in T-ERG over T-fl/fl-ERG organoids	NES	FDR q
1	METABOLISM_OF_RNA	3.16	<0.001
2	CELL_CYCLE_CHECKPOINTS	3.12	<0.001
3	RRNA_PROCESSING	3.06	<0.001
4	RESOLUTION_OF_SISTER_CHROMATID_COHESION	3.01	<0.001
5	RRNA_MODIFICATION_IN_THE_NUCLEUS_AND_CYTOSOL	2.99	<0.001
6	SEPARATION_OF_SISTER_CHROMATIDS	2.98	<0.001
7	CELL_CYCLE	2.96	<0.001
8	DNA_REPLICATION	2.96	<0.001
9	MITOTIC_METAPHASE_AND_ANAPHASE	2.95	<0.001
10	CELL_CYCLE_MITOTIC	2.93	<0.001
11	PROCESSING_OF_CAPPED_INTRON_CONTAINING_PRE_MRNA	2.91	<0.001
12	TRNA_PROCESSING	2.89	<0.001
13	DNA_REPLICATION_PRE_INITIATION	2.88	<0.001
14	MITOTIC_SPINDLE_CHECKPOINT	2.88	<0.001
15	MITOTIC_G1_PHASE_AND_G1_S_TRANSITION	2.88	<0.001
16	MITOTIC_PROMETAPHASE	2.83	<0.001
17	S_PHASE	2.83	<0.001
18	CHROMOSOME_MAINTENANCE	2.82	<0.001
19	G2_M_CHECKPOINTS	2.80	<0.001
20	M_PHASE	2.79	<0.001

B**C****D**

Type	Total # of organoids/cells	% EdU/Cdt1 overlap
T-fl/fl-ERG	10/492	0%
+ERG	12/574	0%

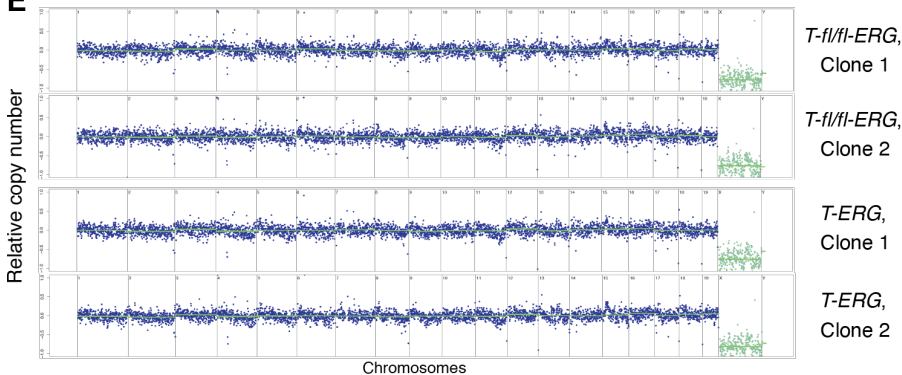
E

Figure S5. Cellular impact of T-ERG in prostate organoids. (A) Top 20 pathways indicated by GSEA NES and FDR q values. **(B)** Example images of cells stained for DNA (DAPI, blue) γ H2AX (red), and

EdU (green) in prostate organoids. Images were taken using a spinning disk confocal microscope with 40X objective magnification. Scale bar: 5 μ m. **(C)** EdU incorporation in cells harboring Cdt1-mCherry. Top pictures: Example images of nuclei with stained EdU (green) and Cdt1-mCherry (red) signals in organoids; white dash lines outline the positions of EdU positive cells. Bottom table: quantification of cells with both EdU and Cdt1 over total amount of assessed cells. Cdt1 is present in G1 phase. **(D)** Expression of apoptosis-related proteins was upregulated upon T-ERG expression. Each bar represents the mean of 2 technical replicates with SEM (error bar). **(E)** All organoids are euploid by the end of all our analyses, determined by low-coverage whole genome sequencing within 30-day growth (within the time frame of all analyses in this paper).

A

RANK	Top 20 Enriched GSEA Pathways in <i>Rad21</i> over <i>Vector</i> in <i>T-ERG</i> organoids	NES	FDR q
1	RESOLUTION_OF_SISTER_CHROMATID_COHESIN	3.01	<0.001
2	MITOTIC_SPINDLE_CHECKPOINT	2.92	<0.001
3	MITOTIC_PROMETAPHASE	2.87	<0.001
4	RETINOBLASTOMA_GENE_IN_CANCER	2.84	<0.001
5	CELL_CYCLE_CHECKPOINTS	2.78	<0.001
6	RHO_GTPASES_ACTIVATE_FORMINS	2.75	<0.001
7	PLK1_PATHWAY	2.74	<0.001
8	CELL_CYCLE_MITOTIC	2.73	<0.001
9	AURORA_B_PATHWAY	2.72	<0.001
10	MITOTIC_METAPHASE_AND_ANAPHASE	2.70	<0.001
11	CELL_CYCLE	2.67	<0.001
12	SEPARATION_OF_SISTER_CHROMATIDS	2.66	<0.001
13	M_PHASE	2.57	<0.001
14	RRNA_PROCESSING	2.55	<0.001
15	ACTIVATION_OF_ATR_IN_RESPONSE_TO_REPLICATION_STRESS	2.55	<0.001
16	DNA_STRAND_ELONGATION	2.51	<0.001
17	FOXM1_PATHWAY	2.48	<0.001
18	DNA_REPLICATION	2.48	<0.001
19	DNA_REPLICATION	2.48	<0.001
20	G1_S_SPECIFIC_TRANSCRIPTION	2.43	<0.001

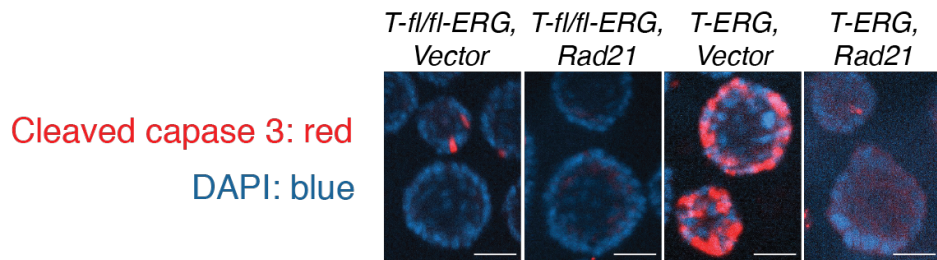
B

Figure S6. Influences of *Tmprss2-ERG* and *Rad21* in cell physiology of prostate organoids. **(A)** Top 20 pathways indicated by GSEA normalized enrichment score (NES). **(B)** Example image of cells stained for DNA (DAPI) and cleaved caspase 3 in prostate organoids. Scale bar: 30 μ m.

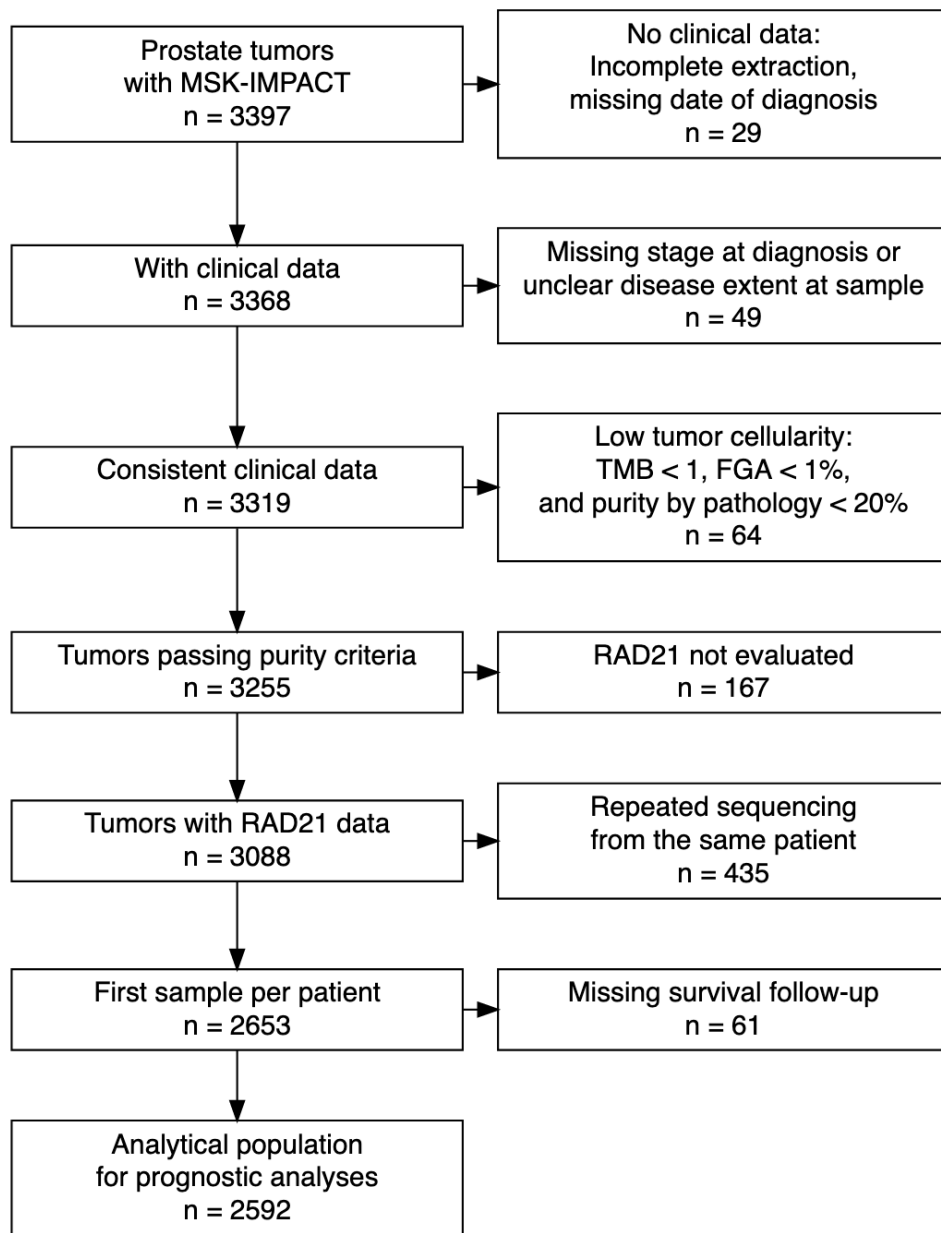


Figure S7. Flowchart of sample and patient inclusion, Memorial Sloan Kettering Cancer Center MSK-IMPACT Prostate Clinical-Genomic Database, 2014–2020.

Supporting text

Additional Methods

RNA Sequencing and Data Analysis

RNA quantification and quality control (QC) were assessed individually using the AATI Fragment Analyzer. 5 replicates of RNA per each sample type were subjected to RNA-seq with QC. Following the template switching reaction, barcoded cDNA samples were pooled, treated with Exonuclease I and cleaned using RNA Ampure beads. Second strand synthesis and PCR amplification were performed using the Advantage 2 Polymerase Mix (Clontech) and the SINGV6 primer (IDT). 12 cycles of PCR were performed, followed by clean up using regular SPRI beads. Successful amplification of cDNA was confirmed using the Fragment Analyzer. Illumina libraries were then produced using standard Nextera tagmentation substituting P5NEXTPT5-bmc primer. Finally, libraries were cleaned using SPRI beads at 1X and quantified using the Fragment Analyzer and qPCR before being loaded for 40X40 paired-end sequencing using the Illumina NextSeq500. After sequencing, quality control on each of the libraries was performed to assess coverage depth, enrichment for messenger RNA (exon/intron and exon/intergenic density ratios), fraction of rRNA reads and number of detected genes using bespoke scripts. The sequencing reads were mapped to the mm10 reference using star/2.5.3a. The negative strand sequences mapped to each gene were counted by rsem/1.3.0. Raw counts were normalized by DESeq2.

Karyotyping Sequencing and Data Analysis

Standard Nextera XT Illumina library prep was applied, and the libraries sequenced with 40bp read length on an Illumina NextSeq500. Sequence reads were trimmed to 40 nucleotides and the resultant reads were aligned to the mouse (mm9) using the BWA (0.7.12) backtrack algorithm (1). HMMcopy (0.1.1) was used to detect copy number alterations by estimating DNA copy number in 500-kb bins controlling for mappability and GC content (calculated by HMMcopy gcCounter) (2).

SI references

1. H. Li, R. Durbin, Fast and accurate short read alignment with Burrows-Wheeler transform. *Bioinformatics* **25**, 1754-1760 (2009).
2. G. Ha *et al.*, Integrative analysis of genome-wide loss of heterozygosity and monoallelic expression at nucleotide resolution reveals disrupted pathways in triple-negative breast cancer. *Genome Res* **22**, 1995-2007 (2012).